

Observation of Quantum Jumps in Superconducting Artificial Atoms with a Josephson Parametric Amplifier



Raffael Rabl
February 2018

Univ.-Prof. Dr. Gerhard Kirchmair
University of Innsbruck

Faculty of Mathematics, Computer Science and Physics
Institute of Experimental Physics
University of Innsbruck

Contents

| | | |
|----------|---|-----------|
| 1 | Introduction | 1 |
| 2 | Concepts | 1 |
| 2.1 | Cavity QED | 1 |
| 2.1.1 | Jaynes-Cummings-model | 2 |
| 2.1.2 | Strong dispersive regime | 2 |
| 2.2 | Quantum Circuits - The LC resonator | 2 |
| 2.3 | Josephson junctions | 2 |
| 2.4 | Transmon - the artificial atom | 2 |
| 2.4.1 | The Cooper-pair-box CPB | 2 |
| 2.4.2 | Transmon regime | 2 |
| 2.5 | A Transmon in a 3D Cavity | 2 |
| 2.6 | Microwave Signals | 2 |
| 2.6.1 | Classical | 2 |
| 2.6.2 | Travelling quantum signals | 2 |
| 2.7 | Josephson-Parametric-Amplifier JPC | 2 |
| 2.7.1 | Josephson ring modulator | 2 |
| 2.7.2 | Scattering matrix | 2 |
| 3 | Characterising the System | 3 |
| 3.1 | Experimental Setup | 3 |
| 3.2 | Cavity Spectroscopy | 3 |
| 3.2.1 | From High Power to Low Power | 3 |
| 3.2.2 | Driving the Transmon | 3 |
| 3.3 | Summary of System Parameters | 6 |
| 4 | Cranking up the Contrast: The Josephson Parametric Amplifier | 7 |
| 4.1 | Travelling Quantum Signals | 7 |
| 4.2 | Operational Principle | 7 |
| 4.2.1 | The Josephson Ring Modulator | 7 |
| 4.2.2 | A Chain of Amplifiers | 7 |
| 4.3 | Tuning Procedure | 7 |
| 4.3.1 | Fluxmaps | 7 |
| 4.3.2 | Controlling the Gain | 8 |
| 4.4 | Testing the JPC SN004 | 10 |
| 4.4.1 | Noise Rise | 10 |
| 5 | Observing Quantum Jumps | 11 |
| 5.1 | Heterodyne Detection Setup | 11 |
| 5.1.1 | Digital Demodulation Scheme | 11 |

| | | |
|-------------------|--|-----------|
| 5.2 | Resolving Quantum States in the IQ-Plane | 12 |
| 5.2.1 | First Measurements | 12 |
| 5.3 | Improving the Contrast | 14 |
| 5.3.1 | Analysing IQ-data: Figures of merit | 14 |
| 5.3.2 | Readout Power Sweep | 17 |
| 5.3.3 | Readout Time | 17 |
| 5.4 | Monitoring the State in Time | 17 |
| 5.5 | Distinguishing three Levels | 19 |
| 5.5.1 | Is the Distribution Thermal? | 19 |
| 5.6 | The Next Step: Pulsed Measurements | 19 |
| 6 | Conclusion & Outlook | 20 |
| Appendix A | Eccosorb Filters | 21 |
| Appendix B | <i>C++ code for digital IQ demodulation</i> | 21 |

List of Symbols

a The number of angels per unit area

JPC Josephson Parametric Amplifier

QED quantum electrodynamics

1 Introduction

Lalalalaaa general introduction whz cQED is awesome for simulation and comp. pleeease write me! Lorem ipsum dolor sit amet, consetetur sadipscing elitr, sed diam nonumy eirmod tempor invidunt ut labore et dolore magna aliquyam erat, sed diam voluptua. At vero eos et accusam et justo duo dolores et ea rebum. Stet clita kasd gubergren, no sea takimata sanctus est Lorem ipsum dolor sit amet. Lorem ipsum dolor sit amet, consetetur sadipscing elitr, sed diam nonumy eirmod tempor invidunt ut labore et dolore magna aliquyam erat, sed diam voluptua. At vero eos et accusam et justo duo dolores et ea rebum. Stet clita kasd gubergren, no sea takimata sanctus est Lorem ipsum dolor sit amet. Lorem ipsum dolor sit amet, consetetur sadipscing elitr, sed diam nonumy eirmod tempor invidunt ut labore et dolore magna aliquyam erat, sed diam voluptua. At vero eos et accusam et justo duo dolores et ea rebum. Stet clita kasd gubergren, no sea takimata sanctus est Lorem ipsum dolor sit amet. Lorem ipsum dolor sit amet, consetetur sadipscing elitr, sed diam nonumy eirmod tempor invidunt ut labore et dolore magna aliquyam erat, sed diam voluptua. At vero eos et accusam et justo duo dolores et ea rebum. Stet clita kasd gubergren, no sea takimata sanctus est Lorem ipsum dolor sit amet.

2 Concepts

In this introductory chapter I present the key concepts, that the reader might find insightful while reading this thesis. I start with a recapitulation of cavity quantum electrodynamics (**cavity QED**) in section 2.1. The central idea of this project is already developed here: determination of the quantum state of the qubit by exploiting the strong dispersive coupling between qubit and cavity. In section 2.5 I discuss, in what manner an artificial atom inside a 3D microwave cavity resembles such a cavity QED system. To gain an intuition about this setup, I give a brief introduction on superconducting quantum circuits. I use the simple example of a LC-oscillator, to describe, how an electronic circuit can be treated by means of quantum mechanics (section 2.2). The most potent element of quantum circuits is the Josephson-junction (section 2.3). Its highly non-linear response, whilst being almost dissipationless, allows for the design of remarkable quantum circuits. Most notably, Josephson-junctions can be used to construct artificial atoms - quantum systems whose intrinsic parameters are controllable over a wide range during the fabrication process (section 2.4). Transition frequencies of these artificial quantum systems are typically in the microwave regime. I introduce a few of the technical terms used in the field of microwave signal processing and describe how weak signals can be described as travelling quantum fields in section 2.6. Finally I present the Josephson-parametric-converter **JPC** in section 2.7. Using this quantum-limited amplifier as first link in the amplification chain of the measurement setup significantly increases the measurement rate and allows the time-resolved observation of quantum jumps.

2.1 Cavity QED

[1]

The theory of quantum electrodynamics (**QED**) describes the interaction between matter and light. Matter is comprised by atoms

The quantized nature of both atoms as well as the electromagnetic field have

The interaction between matter and light can only be understood in

2.1.1 Jaynes-Cummings-model

2.1.2 Strong dispersive regime

2.2 Quantum Circuits - The LC resonator

2.3 Josephson junctions

2.4 Transmon - the artificial atom

2.4.1 The Cooper-pair-box CPB

2.4.2 Transmon regime

2.5 A Transmon in a 3D Cavity

2.6 Microwave Signals

2.6.1 Classical

- Transmission line
- SNR
- Amplifiers: Gain, Noise Temp, Noise figure, ...

2.6.2 Travelling quantum signals

2.7 Josephson-Parametric-Amplifier JPC

2.7.1 Josephson ring modulator

2.7.2 Scattering matrix

3 Characterising the System

3.1 Experimental Setup

3.2 Cavity Spectroscopy

3.2.1 From High Power to Low Power

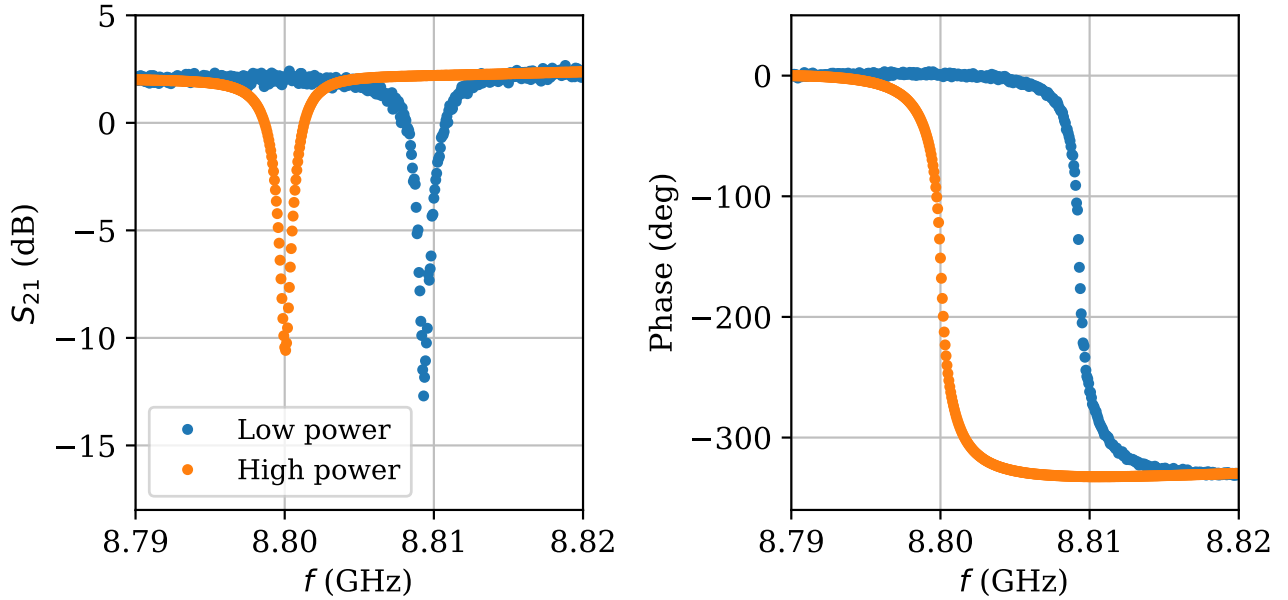


Figure 1: Reflection spectrum of the cavity taken with a VNA for high (blue) and low power (orange). In the low-power-measurement the average excitation of the cavity field amounts to roughly 10 (check this number!) photons. The observed lamb-shift of the resonance frequency is due to the coupling between cavity and transmon.

3.2.2 Driving the Transmon

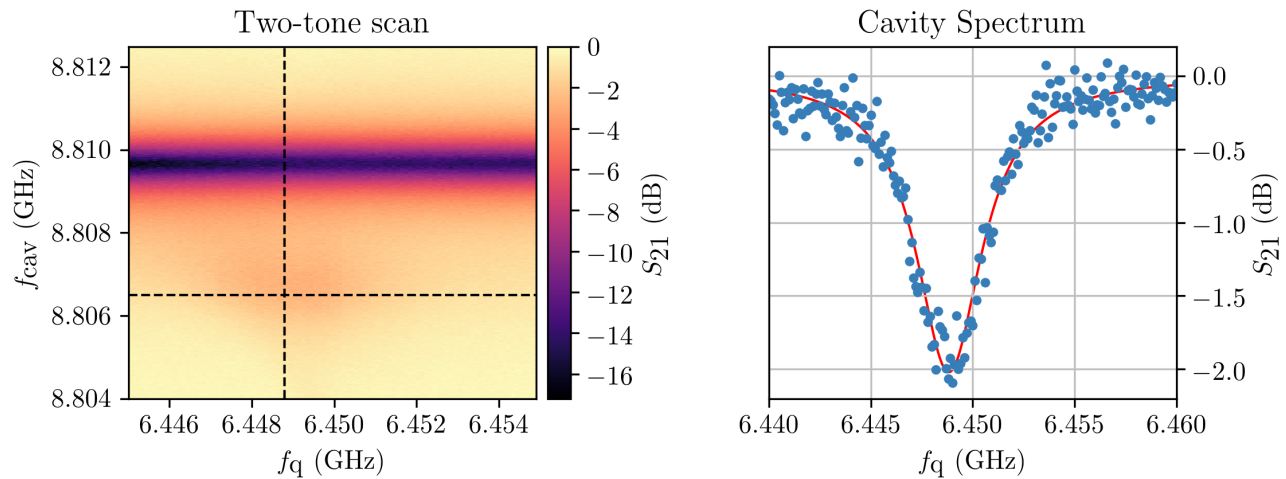


Figure 2: testcaption

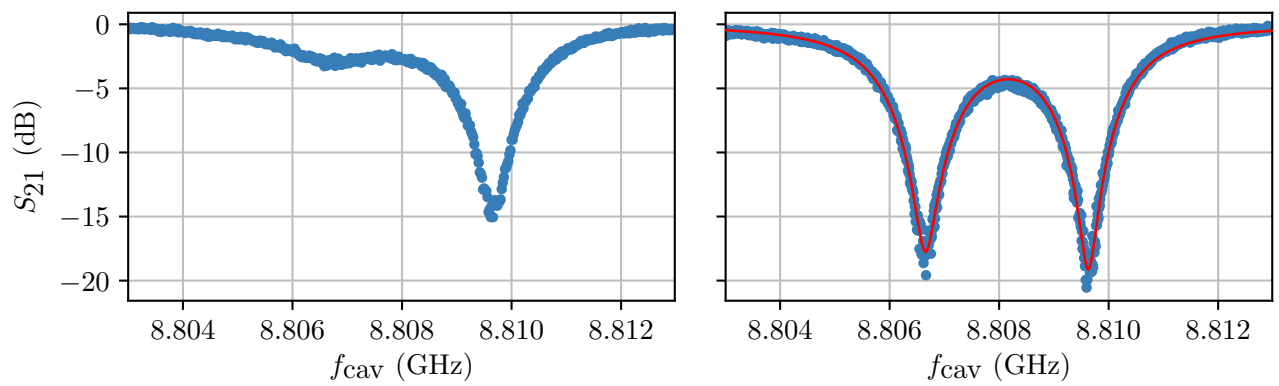


Figure 3: testcaption

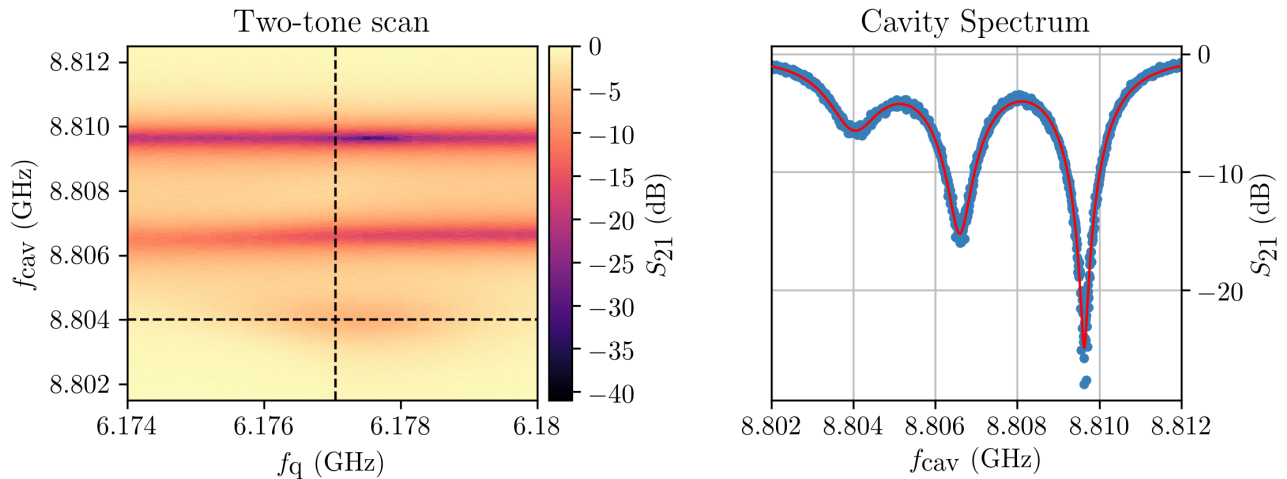
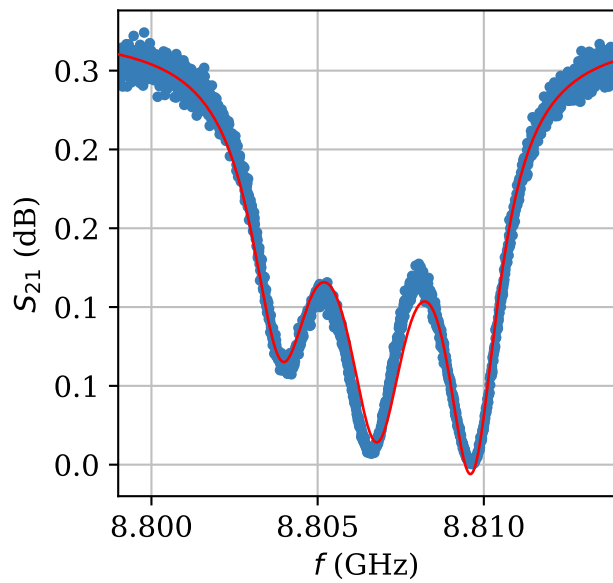


Figure 4: testcaption

Figure 5: Same as above but linear P_{in}/P_{out} data.

3.3 Summary of System Parameters

| Description | Symbol | Value |
|---|--------------------|------------------|
| Cavity when transmon in $ g\rangle$ | $\omega_c^g/2\pi$ | 8.809 641(2) GHz |
| Cavity when transmon in $ e\rangle$ | $\omega_c^e/2\pi$ | 8.806 588(3) GHz |
| Cavity when transmon in $ f\rangle$ | $\omega_c^f/2\pi$ | 8.803 983(3) GHz |
| Dispersive shift | $\chi/2\pi$ | 3.053(5) MHz |
| Cavity decay rate | $\kappa/2\pi$ | 2.096(5) MHz |
| Transmon $ g\rangle \leftrightarrow e\rangle$ transition | $\omega_{ge}/2\pi$ | 6.4500(3) GHz |
| Transmon $ e\rangle \leftrightarrow f\rangle$ transition | $\omega_{ef}/2\pi$ | 6.177(2) GHz |
| Anharmonicity | $\alpha/2\pi$ | 273 MHz |
| Qubit dephasing | Γ | |

Table 1: Experimentally determined parameters of the transmon-cavity-system.

4 Cranking up the Contrast: The Josephson Parametric Amplifier

4.1 Travelling Quantum Signals

4.2 Operational Principle

4.2.1 The Josephson Ring Modulator

4.2.2 A Chain of Amplifiers

4.3 Tuning Procedure

4.3.1 Fluxmaps

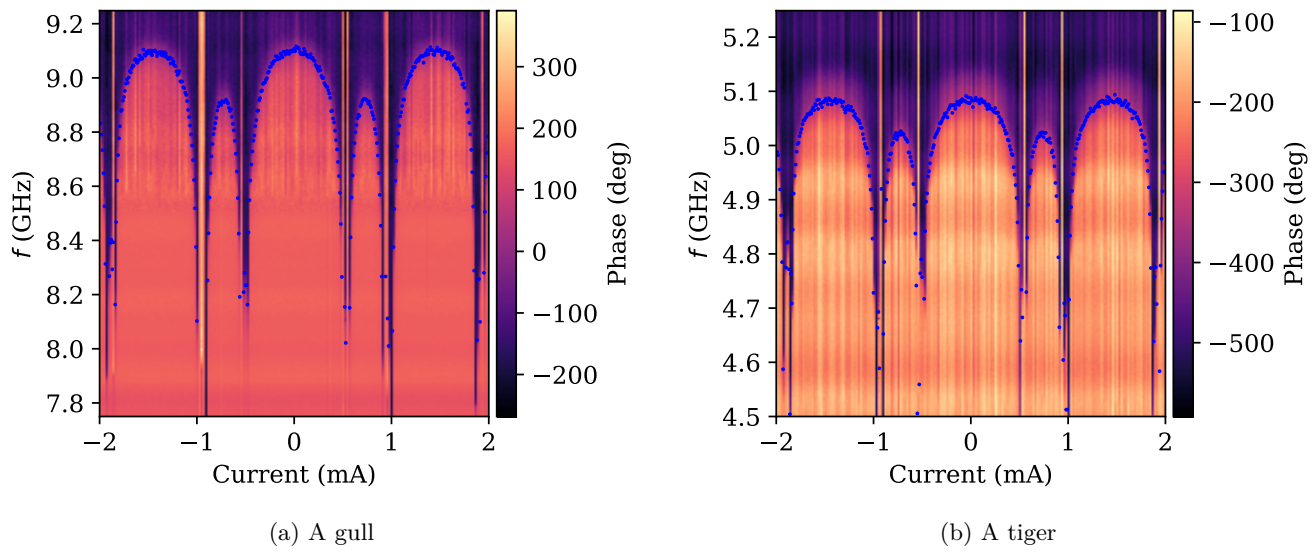


Figure 6: Pictures of animals

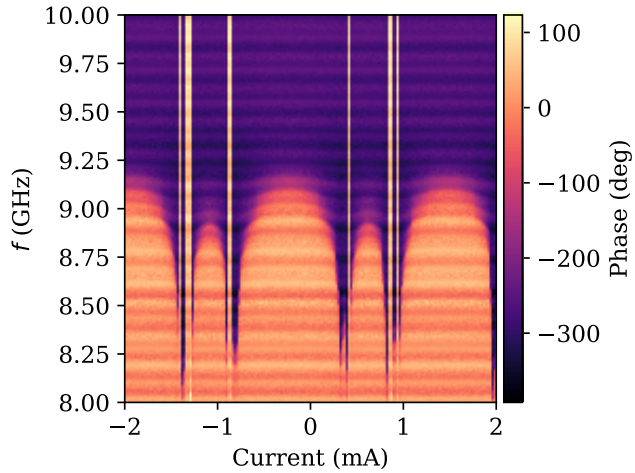
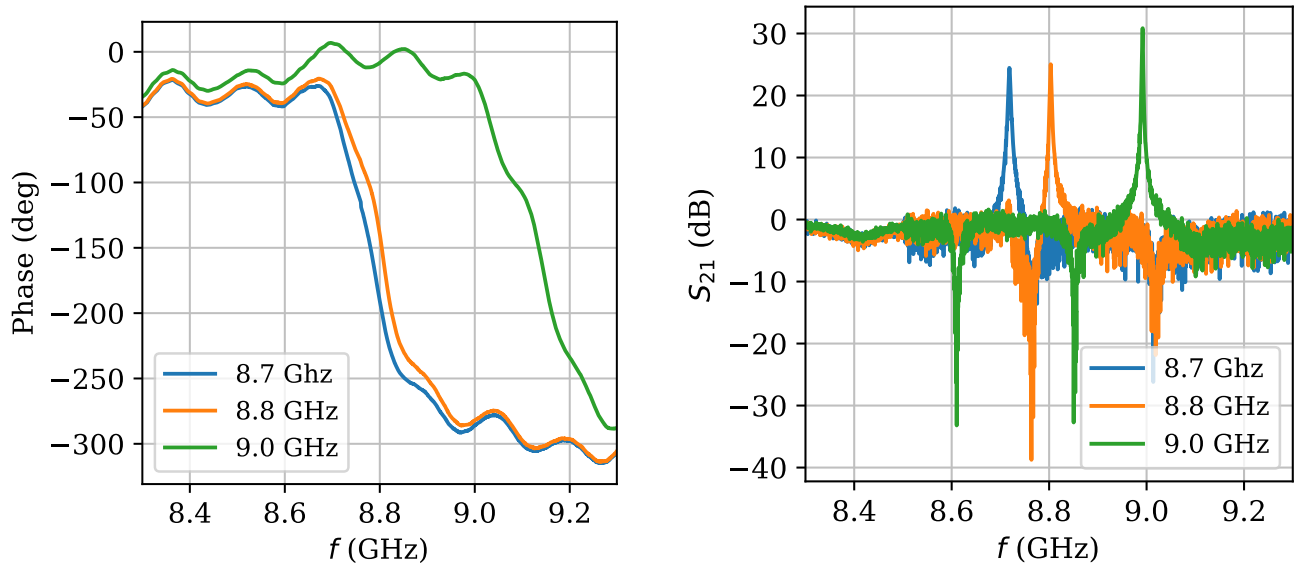


Figure 7: Measured Fluxmap of the JPC SN004.

4.3.2 Controlling the Gain



(a) Phase response of the signal reflected by the JPC signal resonator for three different bias currents while the pump is off.

(b) Magnitude of the reflected signal for the same bias current as in (a) with pump tuned accordingly, to produce a gain. The dips in the data are due to qubits in the waveguide.

Figure 8: Controlling the position of the central JPC gain frequency. The signal-resonator is tuned via the bias current until it covers the desired frequency (a). Then the JPC-pump is turned on and its power is carefully increased (a). The gain should be visible in transmission if the frequency matching condition $\omega_S + \omega_I = \omega_P$ is fulfilled. If no gain appears, the pump has to be set to a slightly different frequency with its power again slowly swept from low to high. A decent guess for ω_P can be obtained from the provided reference fluxmaps 6 for the signal and idler resonator of the JPC.

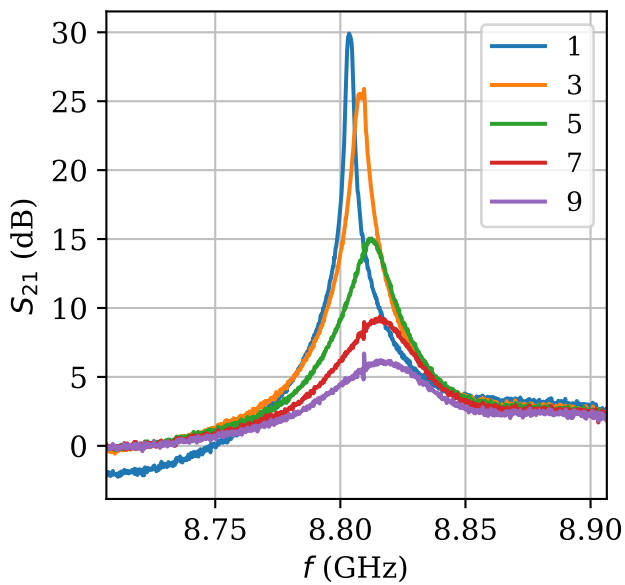
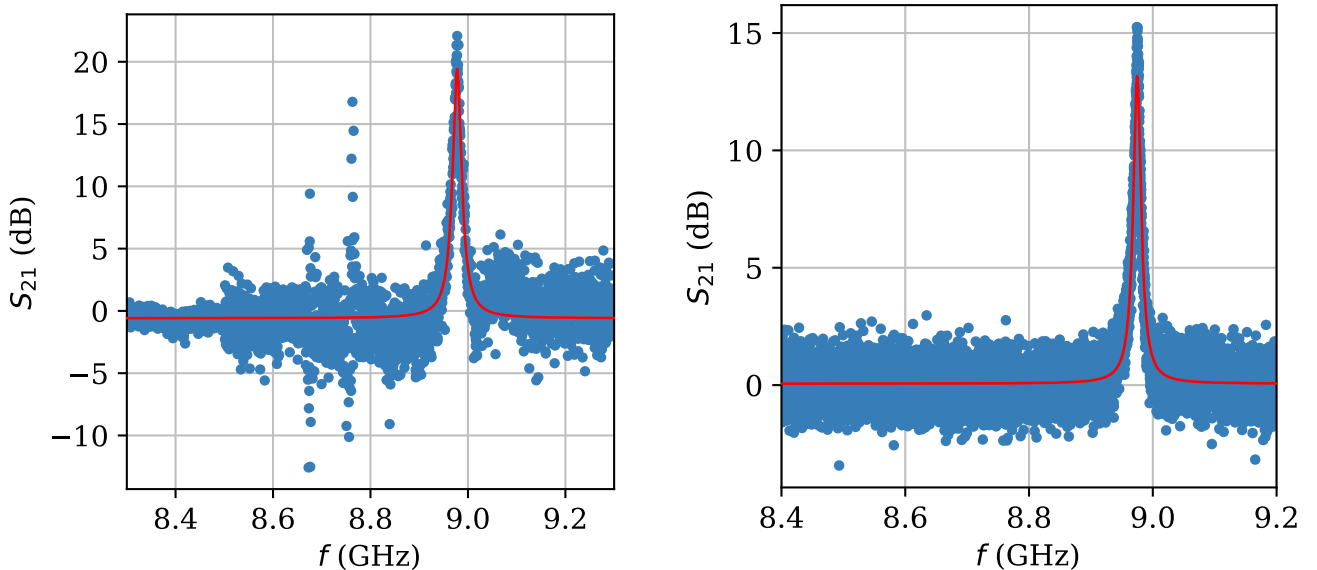


Figure 9: Gain curve of the JPC for different pump powers.

4.4 Testing the JPC SN004

4.4.1 Noise Rise



(a) Calibrated reflection measurement of the JPC. Fitting a lorentzian reveals a gain of 13 dB at 8.974 GHz.

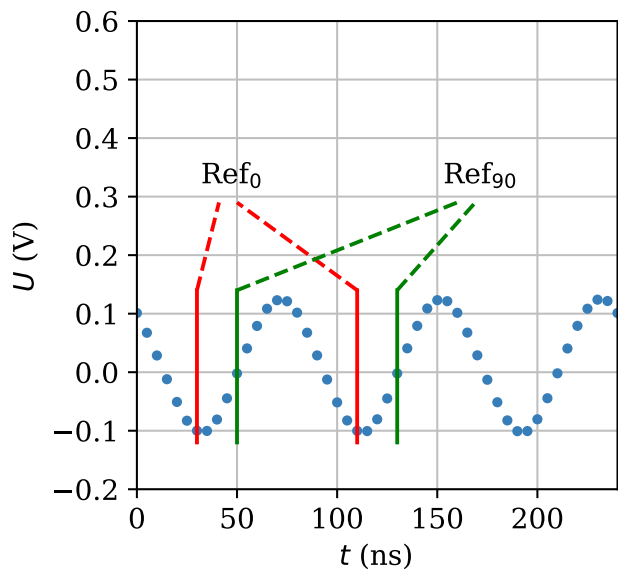
(b) Spectral power density coming out of the signal port of the JPC, measured with a spectrum analyser (subtracted background). The JPC is operated with the same parameters as in (a). The noise added by the JPC is clearly visible.

Figure 10: JPC gain: 20dB, NVR: 13.1dB ... Please measure me again!

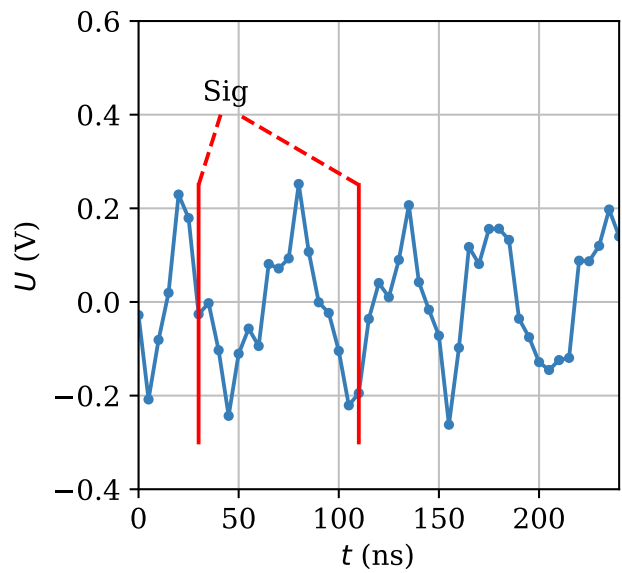
5 Observing Quantum Jumps

5.1 Heterodyne Detection Setup

5.1.1 Digital Demodulation Scheme



(a) caption 111



(b) caption 111

Figure 11: main caption

5.2 Resolving Quantum States in the IQ-Plane

5.2.1 First Measurements

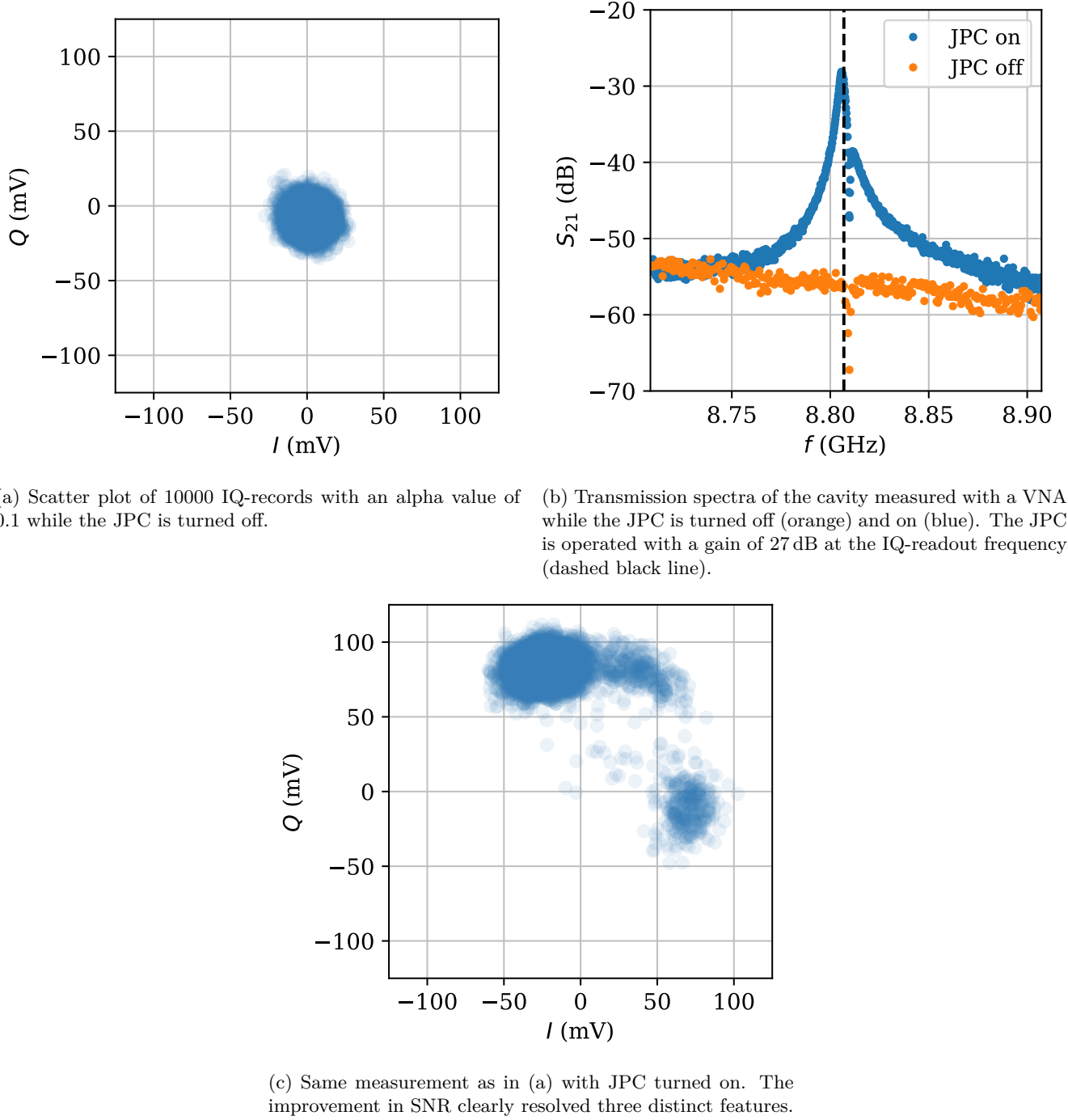


Figure 12: First IQ-measurements with $T_{mes} = 640$ ns at $P_{mes} = 16$ dBm and a probe frequency $f_P = 8.8069$ GHz. Without the JPC the characteristic features, that would indicate the quantum state of the system, remain hidden in the noise (a). Turning on the JPC with the maximum gain frequency tuned to the IQ readout frequency f_P (b) increases the SNR and reveals three distinct spots at which the individual measurement records accumulate (c). Their distribution clearly deviate from the expected gaussian shape. This is due to the high readout-power and hard driving of the JPC.

5.3 Improving the Contrast

5.3.1 Analysing IQ-data: Figures of merit

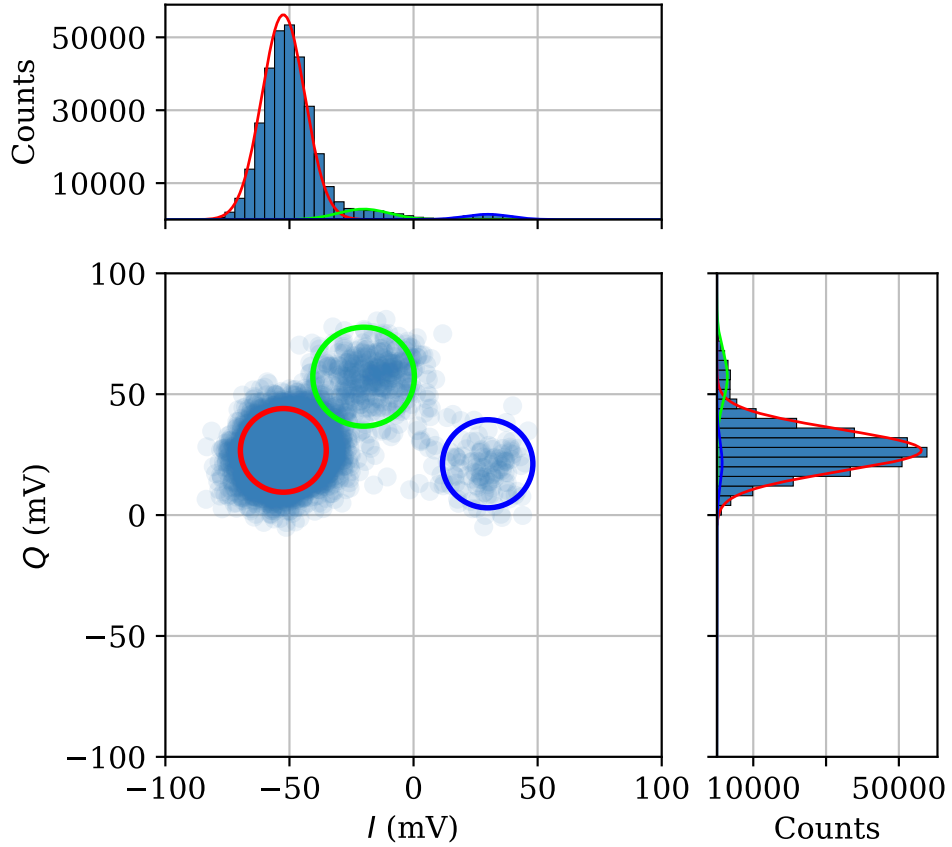
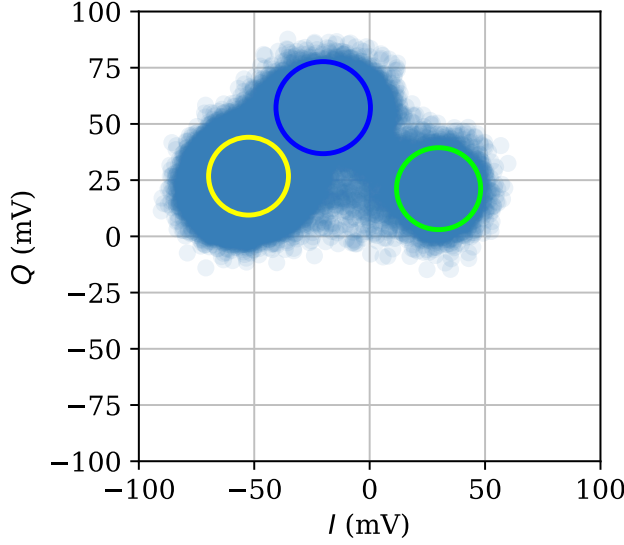
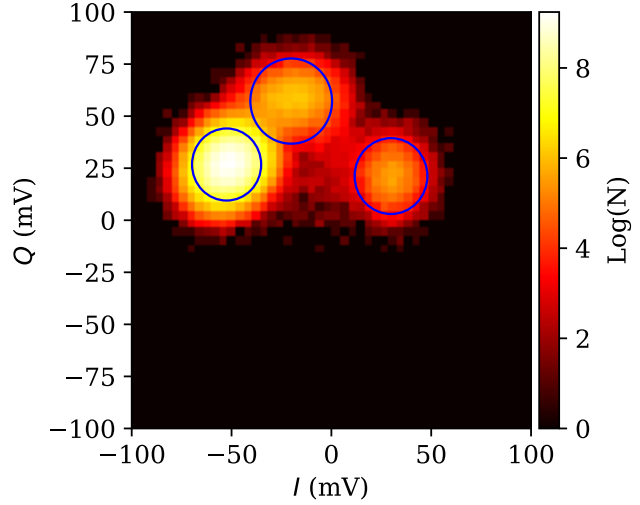


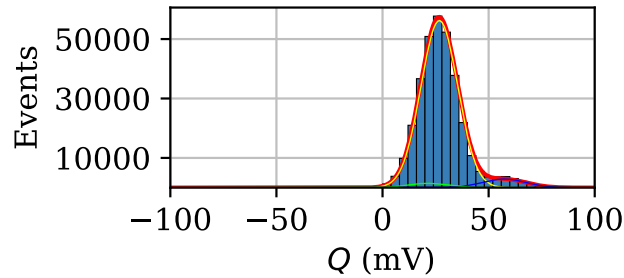
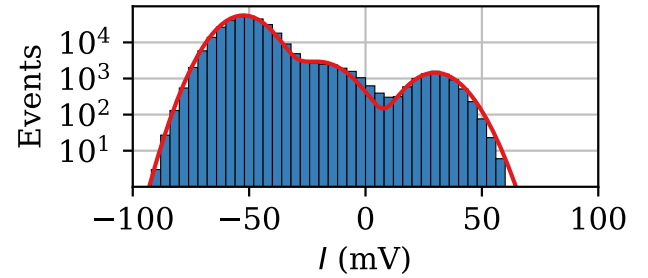
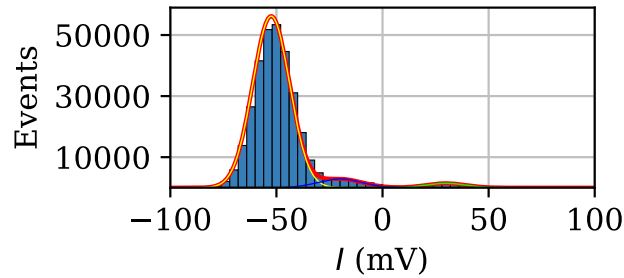
Figure 13: IQ-measurement with $T_{mes} = 640$ ns at $P_{mes} = 24$ dBm and 330000 points. The scatter plot shows the first 10000 data points with an alpha value of 0.1. The circles represent the 2σ -radius of the gaussian profiles obtained by fitting the 2D-histogram as described above. The histograms are computed by binning the I - respectively the Q -component of each individual measurement record of the full data set into 50 intervals of equal length. The coloured lines again show the gaussian profiles of the corresponding disk, as achieved from fitting the 2D-model, but the amplitude is corrected by a scaling factor of $\sqrt{2\pi\sigma^2}$ times the bin-width to account for the projection onto the respective axis.



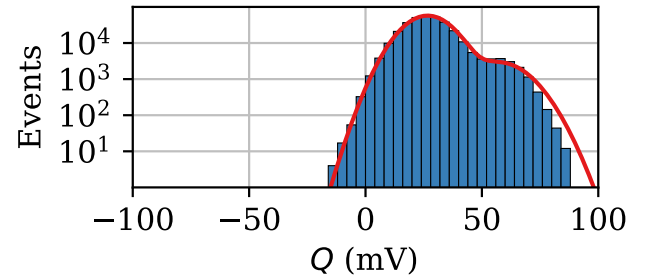
(a) Scatter plot of the IQ-data with 2σ -radius of the fitted gaussian profiles.



(b) Logarithmic histogram of the binned IQ-data.



(c) Cumulative projection of the binned data onto the Q - and I -axis and the gaussian envelopes of the respective disks. The colors are the same as in (a), the sum of the three gaussians is shown in red.



(d) Projection of the logarithmic histogram. Does this even make sense?

Figure 14: IQ-measurement with $T_{mes} = 640$ ns at $P_{mes} = 24$ dBm and 330000 points. In order to quantify the separation and the spread of the disks, that represent the different quantum states, I bin the results onto a 2D-histogram and perform a least-square-fit with the sum of three gaussian profiles.

5.3.2 Readout Power Sweep

5.3.3 Readout Time

5.4 Monitoring the State in Time

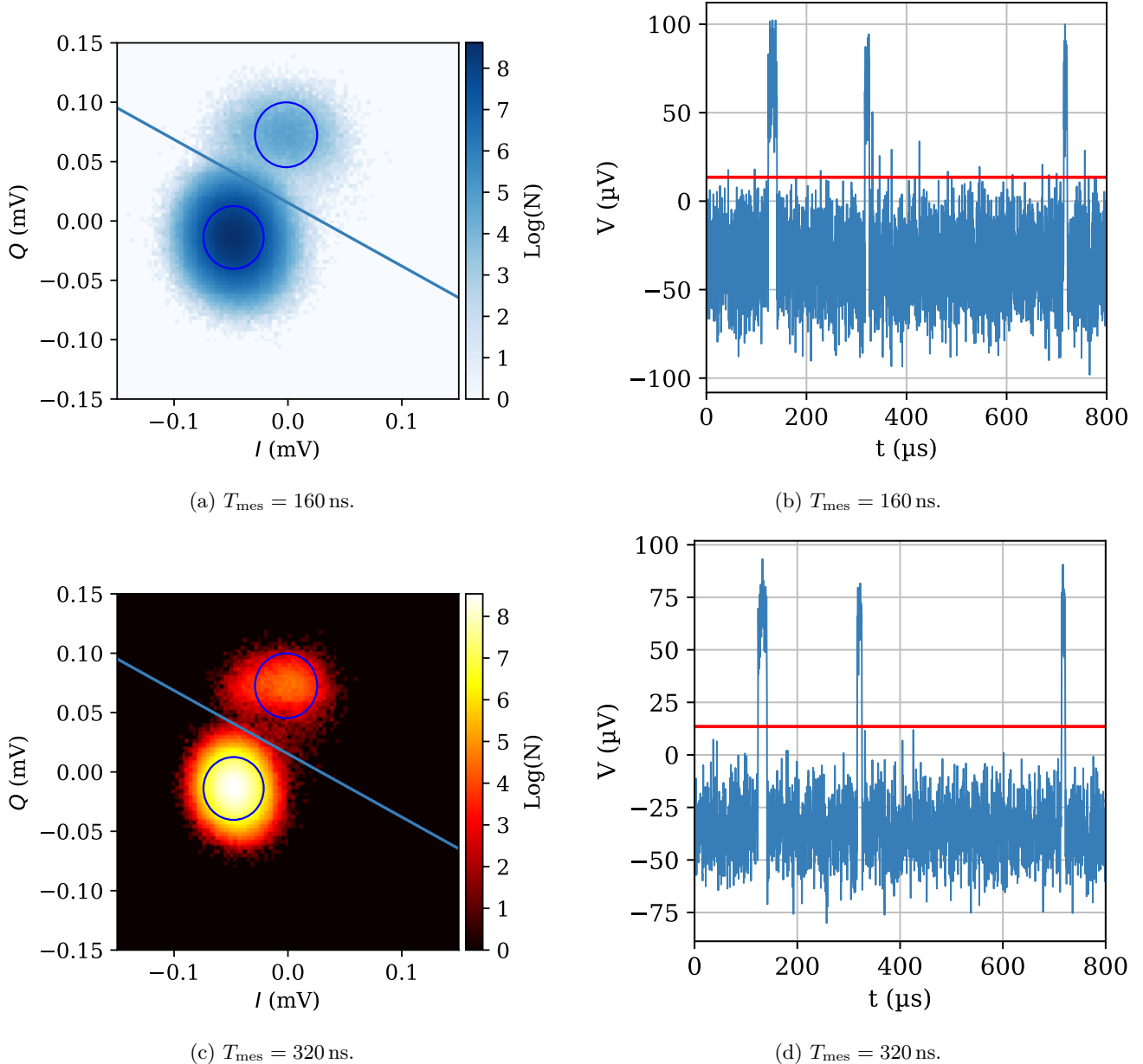


Figure 15: Quantum jump traces for two different measurement times. The blue circles in the IQ plots (a) and (c) show the 2σ -radius of the fitted gaussians. Projecting the data onto the separation line and plotting it in ascending temporal order clearly reveals the instantaneous quantum jumps between the states of the system (b), (d)

5.5 Distinguishing three Levels

5.5.1 Is the Distribution Thermal?

5.6 The Next Step: Pulsed Measurements

6 Conclusion & Outlook

Appendices

A Eccosorb Filters

B *C++* code for digital IQ demodulation

Contents...

References

- [1] Serge Haroche and Daniel Kleppner. Cavity quantum electrodynamics. *Physics Today*, 42(1):24–30, 1989.